Investigation of the resolution enhancement achieved by MIMO Sonar systems

Sven Schröder[1], Ziliang Qiao[2], Dieter Kraus[3], Nils Theuerkauf[4]

[1] *Hochschule Bremen, 28199 Bremen, E-Mail: svschroeder@stud.hs-bremen.de*

[2] *Technische Universität Darmstadt, 64283 Darmstadt, E-Mail: zqiao@stud.hs-bremen.de*

[3] *Hochschule Bremen, 28199 Bremen, E-Mail: Dieter.Kraus@hs-bremen.de*

[4] *ATLAS ELEKTRONIK GmbH, 28309 Bremen, E-Mail: Nils.Theuerkauf@Atlas-Elektronik.com*

Introduction

An active Sonar (sound navigation and ranging) system is a device which uses acoustical waves to detect and locate objects by using the echo principle. It transmits acoustical waves and receives the echo signal reflected from objects, where the receiver often consists of an array with several receiver elements. By using the time delay relation of the received signals the location of the object can be estimated. This procedure is also called conventional beamforming. Because this approach uses a single transmitter antenna and multiple receiver elements this system is called a Single-Input Multiple-Output (SIMO) Sonar. The resolution in range depends on the used probing signal and the angular resolution on the aperture of the receiving antenna. A Multiple-Input Multiple-Output (MIMO) Sonar has more than one transmitter and can transmit multiple probing signals that are uncorrelated or in the ideal case orthogonal to each other, with a broad or omnidirectional beam [1]. The superposition of the backscattered signals are then received and separated from each other by matched filter banks. The output of these matched filter banks are NM signals, where N is the number of receiver elements and M the number of transmitters. With an optimal geometric arrangement of transmitters and receivers, this technique allows to form a virtual array with NM virtual elements, by using only $N+M$ physical transducers. This allows a significant enhancement of the azimuthal resolution without enlarging the physical length of the receiver array [2]. Applications to this technique are high resolution Sonar systems, e.g. for harbor protection. In this paper the basic principle of a MIMO system and the concept of an virtual array is introduced. Also the simulation tool and MIMO signal processing are described. The experimental part of this paper considers the enhancement of resolution of an MIMO array with simulated and in a laboratory environment recorded data.

MIMO Principal

This paper follows the concept of a virtual array. Consider a system consisting of M omnidirectional transmitters and N omnidirectional receivers, where the location of the mth transmitter and nth receiver is given by $\boldsymbol{q}_{T,m}$ and $\boldsymbol{q}_{R,n}$, respectively. The mth transmitter element emits the narrow band waveform $s_m(t)$. With the ideal assumption, that the transmitted waveforms are orthogonal

$$\int s_m(\tau)s_k^*(\tau)d\tau = \delta_{m-k},\ \ m,k = 0,\dots,M-1 \tag{1}$$

these waveforms can be extracted on the receiver side by M matched filters. Therefore the total number of extracted signals equals NM. By assuming a far-field point target, the target response of the mth matched filter of the nth receiver satisfies

$$s_{mn}(t) \propto e^{jk\,\boldsymbol{u}_t^T(\boldsymbol{q}_{R,n}+\boldsymbol{q}_{T,m})},\quad m = 0,\dots,M-1,\quad n = 0,\dots,N-1 \tag{2}$$

where $\boldsymbol{u}_t$ is a unit vector pointing from the Sonar system toward the target, which is located in the origin of the coordinate system [3]. It can be noted that the phase term depends on the location of the transmitters and the receivers. The target responses in (2) are the same as the target responses obtained by a receiving array with NM antenna elements that are located at

$$\left\{\boldsymbol{q}_{R,n} + \boldsymbol{q}_{T,m} \middle| n = 0,\dots,N-1, m = 0,\dots,M-1\right\} \tag{3}$$

This NM-element array is called virtual array. Therefore it is possible to create a NM-element virtual array by only using $N+M$ physical transducers. Introducing the aperture functions of the receivers and the transmitters as discrete linear arrays aligned on the y-axis

$$q_R(y) = \sum_{n=0}^{N-1} \delta(y + nd_R) \tag{4}$$

and

$$q_T(y) = \sum_{m=0}^{M-1} \delta(y + md_T), \tag{5}$$

the aperture function of the virtual array can be expressed as

$$q_V(y) = \sum_{n=0}^{N-1}\sum_{m=0}^{M-1} \delta\big(y + (nd_R + md_T)\big), \tag{6}$$

where d_R is the distance between the receivers and d_T the distance between the transmitters. Furthermore (6) can be formulated as

$$q_V(y) = q_R(y) * q_T(y). \tag{7}$$

To specify the configuration for the transmitter and receiver array a notation for the location of array elements on an equispaced grid with the distance $d = d_R = d_T$,is introduced by

$$q_T = \{1 \quad 0 \quad 0 \quad 1\} \ \text{ and } \ q_R = \{1 \quad 1 \quad 1\} \tag{8}$$

where each entry of the sequence correspondents to the number of transducers on the location in the d-grid. Applying (7), the virtual array is given by

$$q_V = \{1 \quad 1 \quad 1 \quad 1 \quad 1 \quad 1\}. \tag{9}$$

Thus, by the configuration of the transmitter and the receiver the virtual MIMO array with a larger aperture can be obtained.

Relation between transmitted and received signals

Let

$$x_m^+(t) = x_m(t)e^{j\omega_c t} \tag{10}$$

denote the analytic signal transmitted by the mth transmitter. Also, let r_{mk} and r_{nk} be the distances between the mth transmitter element and the kth target and between the nth receiver element and the kth target, respectively. The travel time of the acoustical wave from the transmitter to the target is defined by

$$\tau_{mk} = \frac{r_{m,k}}{c}. \tag{11}$$

Assuming the transmitters to be omnidirectional and the targets to be point scatterers with complex reflection factors $\varrho_k, k = 1, \dots, K$, the analytic signal which is reflected by the kth target can be express by

$$s_k^+(t) = \varrho_k \sum_{m=1}^{M} a_{m,k} x_m(t - \tau_{m,k}) e^{j\omega_c(t-\tau_{m,k})}, \tag{12}$$

where $a_{m,k}$ represents the path loss between the mth transmitter and the kth scatterer. The travel time from the kth target to the nth receiver element is defined by

$$\tau_{n,k} = \frac{r_{n,k}}{c}. \tag{13}$$

Thus supposing omnidirectional receivers, the analytic signal observed at the nth receiver can be describe by

$$\begin{aligned} y_n^+(t) &= \sum_{k=1}^{K} a_{n,k}\, s_k^+(t - \tau_{n,k}) \\ &= \sum_{k=1}^{K} \sum_{m=1}^{M} \{\varrho_k a_{n,k} a_{m,k} \times \\ &\quad \times s_m(t - \tau_{m,k} - \tau_{n,k}) e^{j\omega_c(t-\tau_{m,k}-\tau_{n,k})}\}, \end{aligned} \tag{14}$$

where $a_{n,k}$ represents the path loss between the kth target and the nth receiver. Finally, after quadrature demodulation the complex base band signal is given by

$$\begin{aligned} y_n(t) = &\sum_{k=1}^{K} \sum_{m=1}^{M} \{\varrho_k a_{n,k} a_{m,k} \times \\ &\times s_m\left(t - (\tau_{m,k} + \tau_{n,k})\right) e^{-j\omega_c(\tau_{m,k}+\tau_{n,k})}\}. \end{aligned} \tag{15}$$

MIMO Signal Processing

The signal processing technique which is used in this paper is sketched in Figure 1. The received real band pass signals are quadrature demodulated and match filtered by a matched filter bank with M filters, where the mth filter correspondence to the mth transmitter signal. Therefore the inputs of the beamformer are NM complex base band signals.

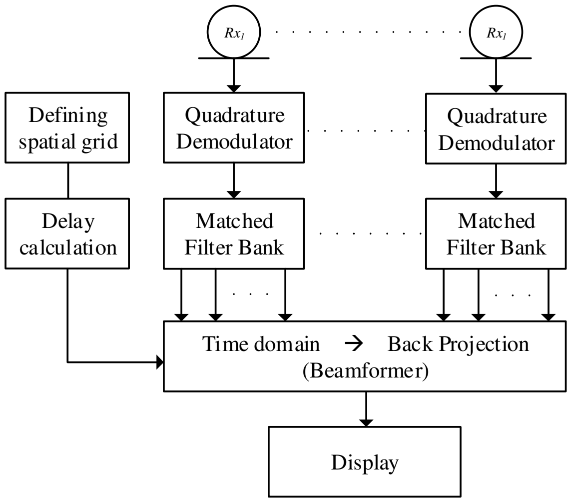

Figure 1: Schematic of the MIMO signal processing

By defining an arbitrary 2-dimensional spatial grid, the theoretical travel time to each grid point for every transmitter/receiver combination is calculated. With the nmth delay calculation, the beamformer projects the nmth matched filter output back on the spatial grid. These NM mapped matched filter outputs are then superimposed to get the beamformer output.

Simulation tool

The signal generation is based on the calculation of the travel time of an acoustical wave form the mth transmitter to the kth scatterer and back to the nth receiver as it is sketched exemplary in Figure 2.

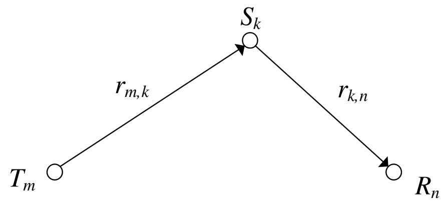

Figure 2: Path of the acoustical wave from transmitter to receiver.

Thus, NMK possible paths exist, where K is the number of scatterers. The travel time of each path can be calculated by

$$\tau_{n,m,k} = \frac{r_{m,k} + r_{n,k}}{c}. \tag{16}$$

The generated transmitter signals $x_m(t)$ are shifted by the time they need for the travel path. This time delay is divided in a sample- and subsample-delay. The sample-delay is defined by

$$\check{\tau}_{n,m,k} = T_s \left\lfloor \frac{\tau_{n,m,k}}{T_s} \right\rfloor = T_s l_{n,m,k} \tag{17}$$

where T_s denotes the sample period and $\lfloor \cdot \rfloor$ the Gaussian-brackets. The subsample-delay is given by

$$0 \leq \tilde{\tau}_{n,m,k} = \tau_{n,m,k} - \check{\tau}_{n,m,k} \leq T_s. \tag{18}$$

After introducing the propagation loss $a_{n,m,k} = a_{n,k} a_{m,k}$ the nth receiver signal can be expressed by

$$\begin{aligned} y_n(lT_s) \quad = \quad & \sum_{m=1}^{M} \sum_{k=1}^{K} a_{n,m,k}\, \varrho_k \times \\ & \times x_m\left(\left(l - l_{n,m,k}\right)T_s - \tilde{\tau}_{n,m,k}\right). \end{aligned} \tag{19}$$

Experimental results for simulated and real data

In this paper the considered setup consists of a line array of N receivers and M transmitters, where the receivers are aligned on the y-axis in the center of the coordinate system. The receiver array consist of $N = 37$ transducers which are spaced equidistantly with a distance between two elements of $d_R = 2.5$ cm. The $M = 2$ transmitters are located at the ends of the receiver array underneath the first and last receiver element with a distance of $d_T = 0.9$ m.

Simulation of a far-field scenario

The first simulation considers a far-field scenario with two scatterers with an angular separation of either $\Delta\beta_1 \cong 4.8°$ and $\Delta\beta_2 \cong 2.4°$, cf. Figure 3 a) and b). The simulation is done with an LFM up- and down-sweep ($f_c = 6.92$ kHz, $B = 2$ kHz, $T = 10$ ms). In [4] other signal types are investigated for MIMO systems. The simulation considers four different arrays: A SIMO array (receiver aperture length of L_{R1} = 92.5 cm), an ideal MIMO array (sequential transmitting), a real MIMO array (simultaneous transmitting) and a large SIMO array (receiver aperture length of $L_{R2} = 1.825$ m) which serves as a benchmark. The angle $\Delta\beta_1$ has been chosen such that the lowering between both scatterers is -3 dB for the SIMO array as a heuristic criterion. The angle $\Delta\beta_2$ is chosen such that the large SIMO array has a lowering of -3 dB between both scatterers. The results in Figure 3 show that the ideal MIMO array with perfect signal separation (sequential transmitting) can reach the azimuthal resolution of the large SIMO array. If the signals are not perfectly uncorrelated as given for the used LFM up- and down sweep and if they are transmitted simultaneous, the array has slightly less azimuthal resolution.

Simulation and Experiment of an near-field scenario

This test includes a laboratory experiment and its comparative simulation. In the experiment two scatterers are positioned in front of the MIMO array (cf. Figure 4), such that the $\Delta\beta_{\mathrm{Exp}} \approx \Delta\beta_2$ in order to be comparable to the simulation of the far-field scenario. Also in the experiment and corresponding simulation both transmitters are sending simultaneous. Figure 5 provides the results of the small SIMO array. As predicted the scatterers cannot be resolved. Figure 6 shows the experimental and simulation results for a MIMO array. As in the far-field scenario both targets can be resolved.

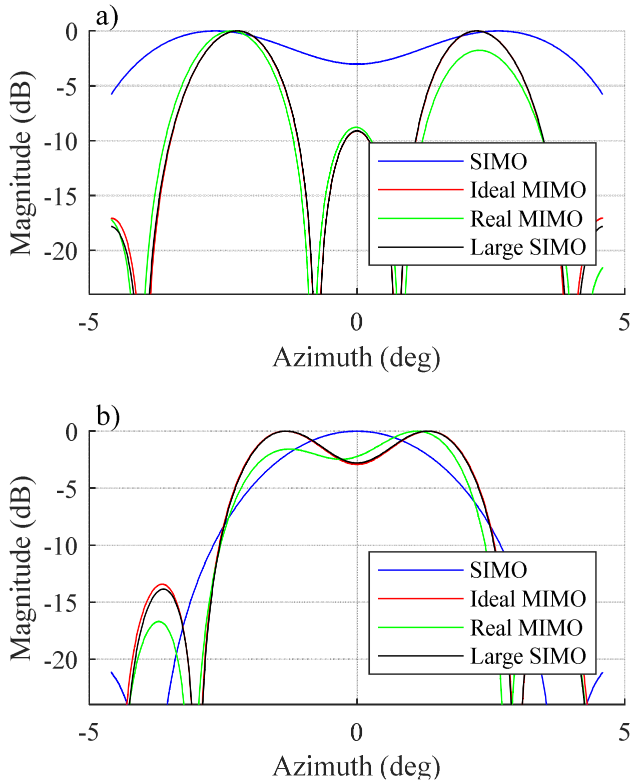

Figure 3: Results of a far-field simulation with a broad-band signal (LFM with $\boldsymbol{f_c} = \mathbf{6.92}$ kHz, $\boldsymbol{B} = \mathbf{2}$ kHz, $\boldsymbol{T} = \mathbf{10}$ ms) and two scatterers with an included angle of $\Delta\boldsymbol{\beta_1}$ in Subfigure a) and $\Delta\boldsymbol{\beta_2}$ in Subfigure b).

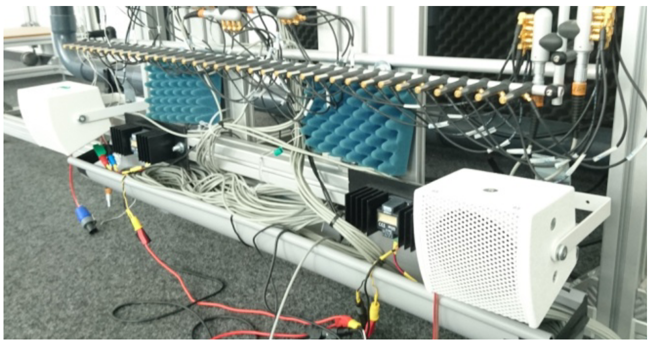

Figure 4: MIMO array in experimental setup

Conclusions

In this paper the resolution enhancement achieved by MIMO Sonar systems has been considered. It could be shown that the theoretical predictions of the virtual array concept are coincident with the observation in the far-field simulation as far as the transmitter signals can be separated by the matched filter bank. Therefore it could be shown that the performance of a MIMO System greatly depends on the cross-correlation of the transmitter signals. The near-field experiment shows a higher resolution enhancement as predicted. This indicates that there are effects in a real environment which have a positive influence on the performance of the system.

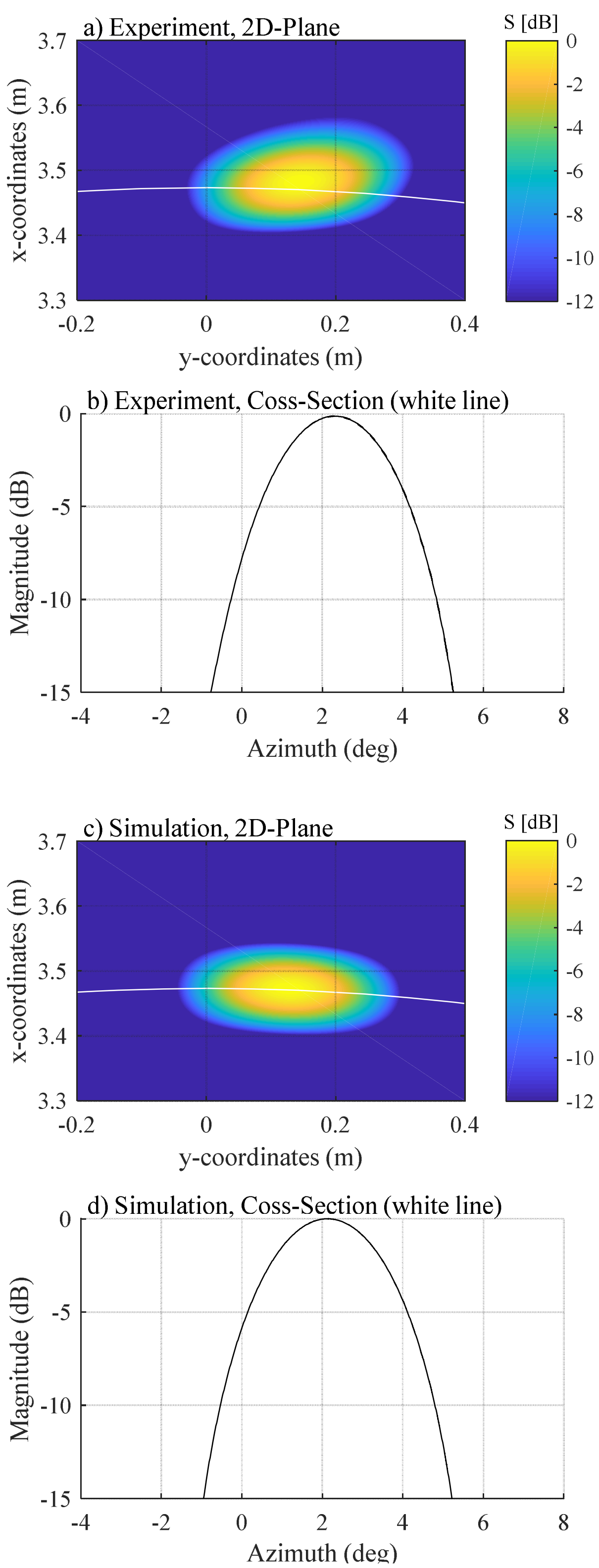

Figure 5: Comparison between the experiment and simulation for a standart SIMO-System with two scatterers, which are not resolvable.

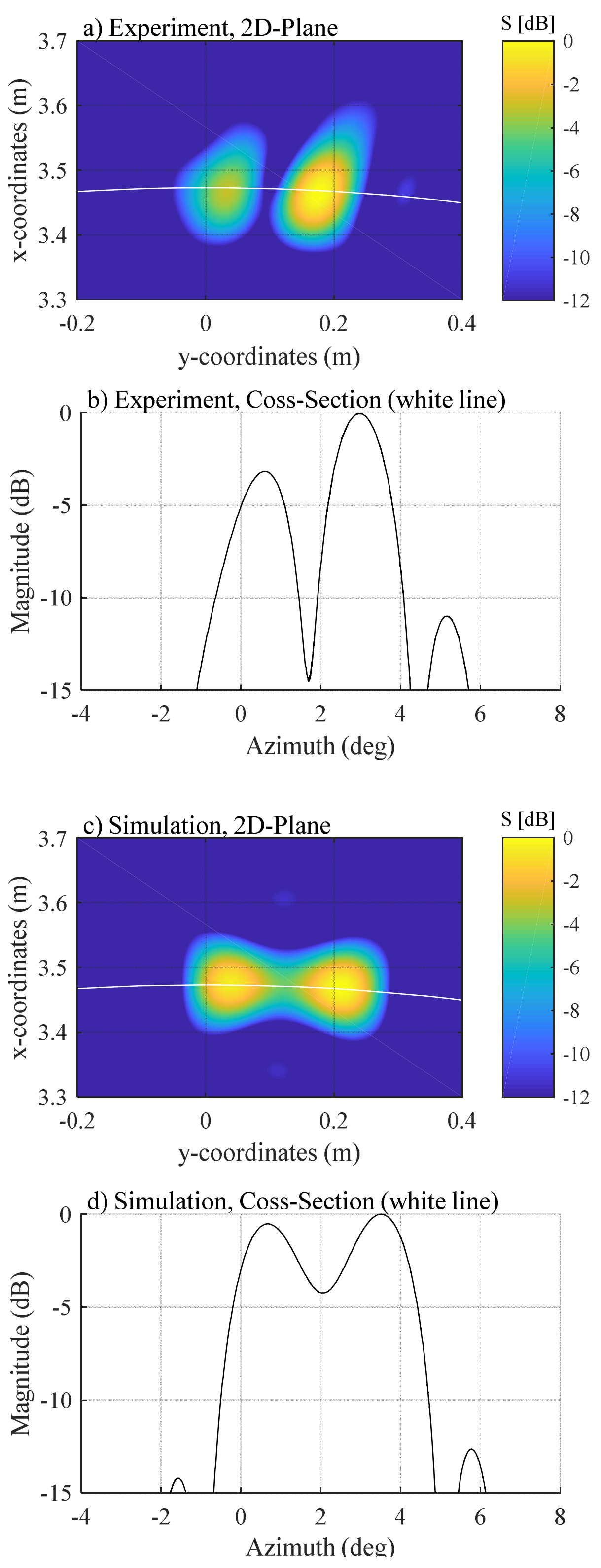

Figure 6: Comparison between the experiment and simulation for the MIMO-System with two scatterers.

Literature

[1] Li, J.; Stoica, P.; Xie, Y.: On Probing Signal Design for MIMO Radar; Proc. 40th Asilomar Conf. Signals, Syst. Comput. Pacific Grove, CA, pp. 31–35, 2006.

[2] Li, J.; Stoica, P.: MIMO Radar with Colocated Antennas, IEEE Signal Processing Magazine, 2007.

[3] Li, J.; Stoica, P.: MIMO Radar Signal Processing, WILEY, 2009.

[4] Schröder, S.: Development and evaluation of a numerical simulation environment for a Multiple-Input Multiple-Output Sonar, Hochschule Bremen, 2017.